

Al–Co–W fusion diagram in the Co–CoAl–W part

G. DMITRIEVA^{1*}, V. VASILENKO¹, I. MELNIK¹

¹ Department of Phase Equilibria, G.V. Kurdyumov Institute for Metal Physics,
National Academy of Sciences of Ukraine, Vernadsky Blvd. 36, 03142 Kyiv, Ukraine

* Corresponding author. E-mail: vvi@imp.kiev.ua

Received November 4, 2008; accepted December 29, 2008; available on-line March 19, 2009

The fusion diagram of the Al–Co–W system in the Co–CoAl–W part was drawn using optical light, differential thermal, X-ray diffraction and electron microprobe analysis data. The alloys were prepared by arc melting. No ternary intermediate phase was found in this partial system above 900°C. The phase equilibria between CoAl and W were established with the peritectic reaction $L+W \leftrightarrow \text{CoAl}$ at 1650°C. The Co–CoAl–W fusion diagram has two isothermal three-phase fields corresponding to four-phase invariant reactions with participation of liquid: $L \leftrightarrow \text{Co} + \text{CoAl} + \text{Co}_7\text{W}_6$ (1380°C) and $L+W \leftrightarrow \text{Co}_7\text{W}_6 + \text{CoAl}$ (1490°C). The solidus and liquidus surface projections and the vertical sections for 75 at.% Co and equiatomic Al and W are presented and compared with the isothermal sections at 1200°C and 900°C reported earlier.

Phase equilibria / Solubility / Fusion diagram / Solidus / Liquidus

Introduction

Aluminium and tungsten are often used as alloying elements in cobalt-base alloy industry. The Al–Co–W phase diagram in the Co-rich part is thus of fundamental importance for practical applications, but up to date it has not been constructed. The similarity of the crystal structures of the compound CoAl (prototype CsCl) and tungsten (prototype α -Fe) makes probable the existence of phase equilibria between these two phases, and that was effectively found in this research. Therefore the investigation of the Co-rich part of the phase diagram of the Al–Co–W system may be cut at ~40 at.% Al, near CoAl. Another compound that takes part in the fusion diagram is Co_7W_6 . The WCoAl compound (prototype MgZn_2) [1] could not be found in the Co–CoAl–W system. The aim of this research was to investigate the phase equilibria in the solid-liquid state and to plot the fusion diagram of the Al–Co–W system in the Co–CoAl–W part. Isothermal sections at 1200°C and 900°C were recently investigated [2,3].

Experimental

Alloys of different compositions were prepared from high-purity metals: Co (99.98 wt.%), Al (99.995 wt.%) and W (99.93 wt.%) by arc melting, using a non consumable W electrode on a water-cooled copper hearth under high-purity argon atmosphere gettered by Ti/Zr. The alloys were prepared as 20 g ingots. The compositions of the alloys are given in Table 1. The

weight losses for all alloys were negligible, less than 0.2%; chemical analyses were carried out for most of the alloys. The ingots were investigated in the as-cast state.

Differential thermal analysis (DTA) was performed using VDTA-8M3. The heating and cooling rates were 60°C/min. Al_2O_3 crucibles were used. The temperatures of phase transformations were measured using the heating curves. Solidus temperatures were measured with accuracy $\pm 10^\circ\text{C}$. Fe- K_α radiation X-ray diffraction (XRD) was used to determine phase composition of the alloys. The microstructure of the samples was investigated by standard techniques. In most cases the samples were etched with a mixture of 5 drops of HNO_3 , 10 drops of HF and 20 ml H_2O . The chemical composition of the phases and the structural constituents of the alloys were determined by quantitative electron probe microanalysis (EPMA) techniques on a Superprobe 733 (JEOL LTD, Tokyo, Japan) device, employing pure Co, Al and W as reference materials. Errors in the measurements were about ± 0.5 at.%.

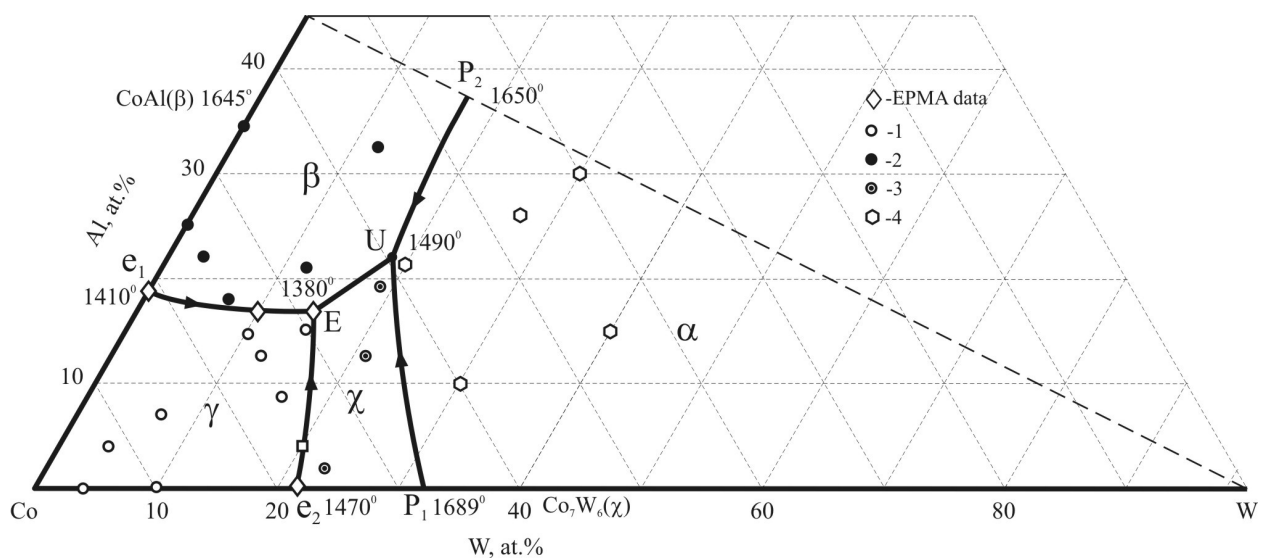
Result and discussion

The binary systems

The binary boundary systems Al–Co and Co–W are essentially accepted as presented in [4-8]. As follows from the present investigation of experimental data, the

Table 1 DTA, MSA, EPMA, TRD data for alloys of the Co–CoAl–W system.

Alloy composition, at.%			Solidus temperature, °C	Liquidus temperature, °C	Primarily crystallized phase	Phase composition at subsolidus temperature
Al	Co	W				
4	96	–	1490	–	Co	Co
14	86	–	1430	1450	Co	Co+(CoAl)
25	75	–	1410	1490	CoAl	Co+CoAl
35	65	–	1540	1560	CoAl	CoAl
–	86	14	1480	–	Co	Co+Co ₇ W ₆
–	75	25	1470	1600	Co ₇ W ₆	Co+Co ₇ W ₆
4	92	4	1490	1510	Co	Co
7	86	7	1470	1495	Co	Co
13.5	79	7.5	1390	–	Co	Co+CoAl
6.5	74.9	18.6	1400	1500	Co	Co+Co ₇ W ₆
2	75	23	1440	1560	Co ₇ W ₆	Co+Co ₇ W ₆
12.5	75	12.5	1380	1450	Co	Co+CoAl+Co ₇ W ₆
15	75	10	1380	1450	Co	Co+CoAl+Co ₇ W ₆
15	70	15	1390	–	(Co)	Co+CoAl+Co ₇ W ₆
19.2	61.8	19	1385	1480	CoAl	CoAl+Co ₇ W ₆
32	55.7	12.3	1495	–	CoAl	CoAl+Co ₇ W ₆
22	74.9	3.1	1390	1470	CoAl	Co+CoAl
14	46	40	–	–	Co ₇ W ₆	Co+CoAl+Co ₇ W ₆
21	66.6	12.4	1380	–	CoAl	Co+CoAl+Co ₇ W ₆
21	57.3	21.7	1450	1500	CoAl	CoAl+Co ₇ W ₆
14	46	40	1490	–	W	W+Co ₇ W ₆ +CoAl
26	47.1	26.9	1490	1610	W	W+CoAl+Co ₇ W ₆
8.5	75.7	15.8	1400	1485	Co	Co+Co ₇ W ₆
30	40	30	1650	–	W	W+CoAl
–	65	35	1480	–	W	W+Co ₇ W ₆
18.5	75.2	6.3	1385	1410	CoAl	Co+CoAl

**Fig. 1** Liquidus surface projection of the Al–Co–W system in the Co–CoAl–W part. 1: primary Co-base phase (γ), 2: primary CoAl (β), 3: primary Co₇W₆ (χ), 4: primary W-base phase (α).

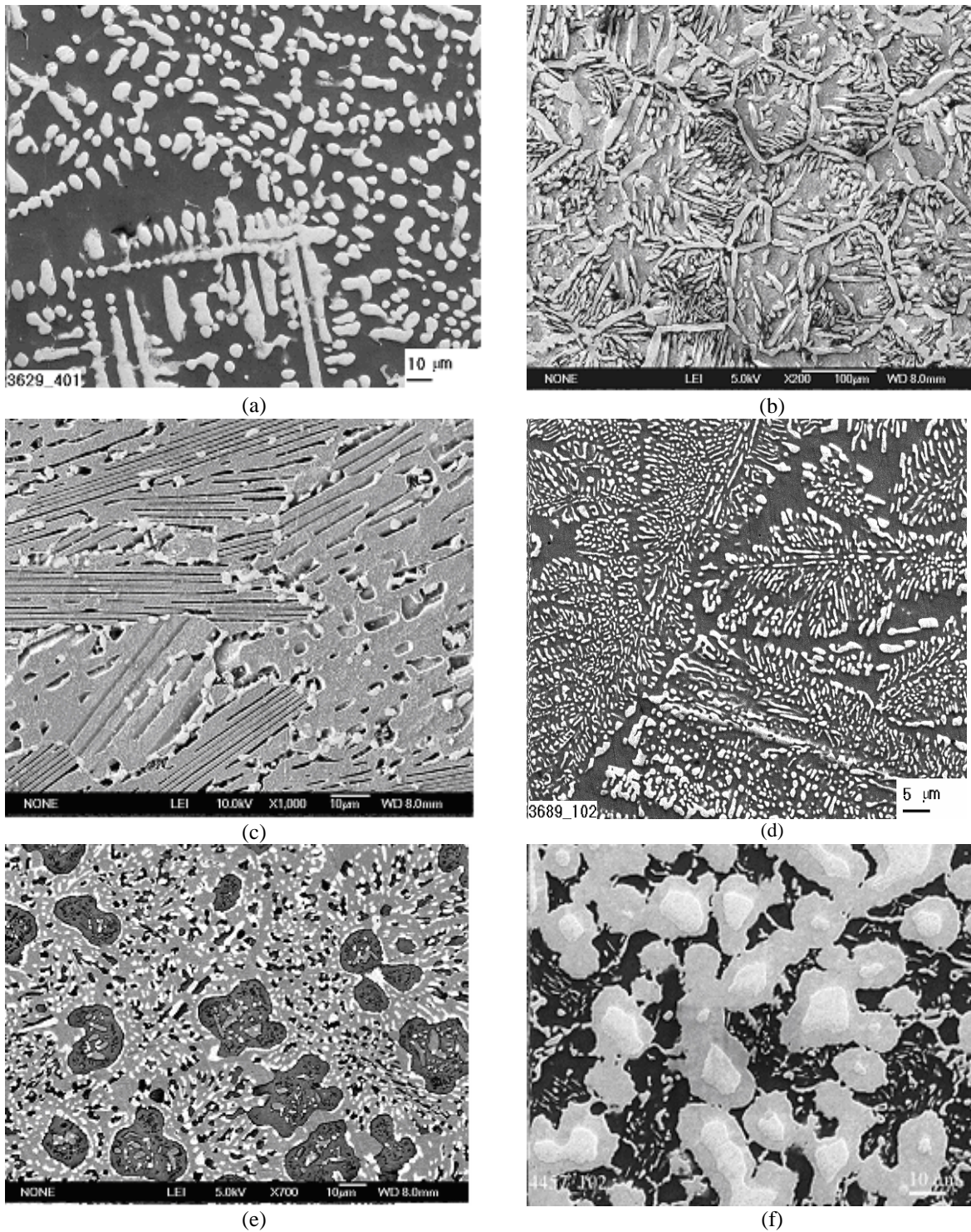


Fig. 2 Microstructures of Co-rich Al–Co–W as-cast alloys, EPMA absorption micrograph; (a) 42Co–28.6Al–29.4W: primary white grains of W-base solid solution in global measurement CoAl; (b) 67Co–21Al–12W: primary light CoAl at the boundaries and inside grains, grey Co-base solid solution and small white W inside the grains too; (c) 75.4Co–18.5Al–6.3W: eutectic Co+CoAl (e_1); (d) 75Co–6.5Al–18.5W: eutectic Co+Co₇W₆ (e_2); (e) 69.9Co–15.3Al–14.8W: ternary eutectic (E) (deep etching); (f) 47.1Co–26Al–26.9W: primary white grows of W-base solid solution surrounded by the grey compound Co₇W₆ and the CoAl base phase.

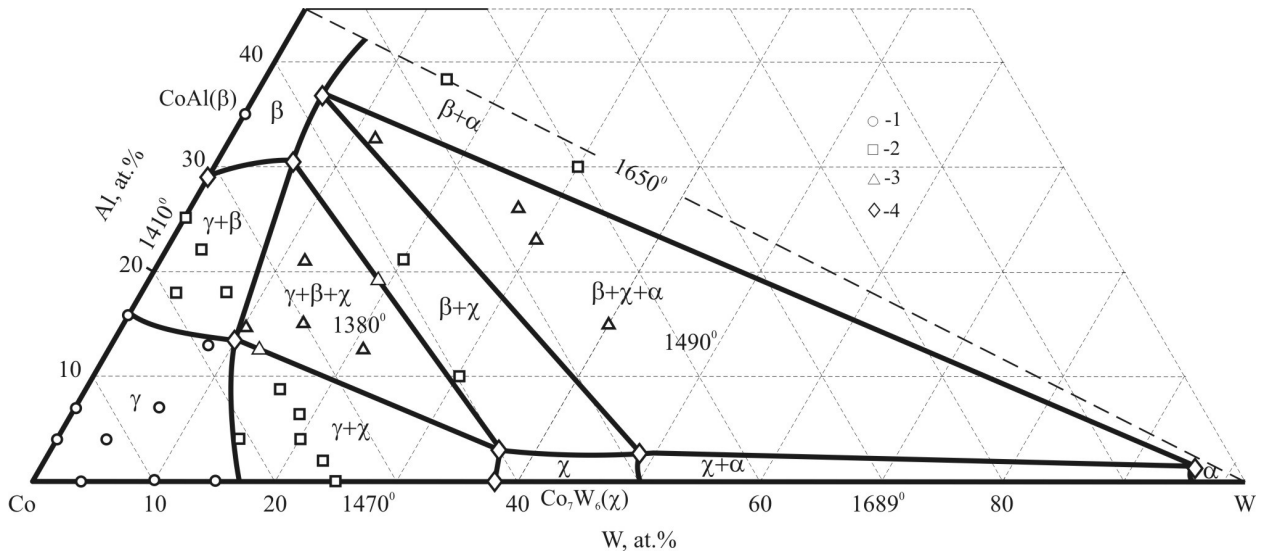


Fig. 3 Solidus surface projection of the Al–Co–W system in the Co–CoAl–W part. 1: single-phase alloys, 2: two-phase alloys, 3: three-phase alloys, 4: EPMA data.

value 1410°C is preferred for the eutectic $L \leftrightarrow \text{Co} + \text{CoAl}$. The maximal solubility of aluminium in cobalt was confirmed to be 14.7 at.% at 1200°C and 11.5 at.% at 900°C (EPMA). The CoAl solidus field on the Co-rich side extends to 29 at.% Al at 1410°C (DTA). The cobalt solid solution contains 15.7 at.% Al at the eutectic temperature.

In the present investigation the experimental data for binary Co–W alloys confirmed 1470°C and 21.6 at.% W for the eutectic reaction and the tungsten content in Co_7W_6 was determined as 39.5 at.% in the limiting alloy at 1470°C.

The ternary system

The phase equilibria in the region of investigation are characterized by the absence of any ternary compound according to the XRD data. The fusion diagram of the Co–CoAl–W system was constructed for the first time in this work.

Liquidus and solidus surfaces

The experimental data for selected as-cast alloys, which were used to plot the fusion diagram of the Co–CoAl–W partial system are presented in Table 1. The liquidus surface projection is shown in Fig. 1.

The primary formation field of the W-base solid solution (s.s.) is the broadest one in the fusion diagram and is delimited by the line WP_1UP_2 . The position of the point P_2 in the fusion diagram was determined according to DTA and microstructure data and was treated as corresponding to the peritectic reaction $L + \text{W} \leftrightarrow \text{CoAl}$ at 1650°C. The microstructure of a two-phase ternary as-cast alloy containing W-base s.s. and CoAl is shown Fig. 2a.

The CoAl primary formation field is delimited by the line e_1EUP_2 . The microstructure of an alloy in this

field is shown in Fig. 2b. The primary solidification of the Co_7W_6 compound takes place in the field delimited by the loop e_2EUP_1 .

The peritectic reactions $L + \text{W} \leftrightarrow \text{CoAl}$ at 1650°C and $L + \text{W} \leftrightarrow \text{Co}_7\text{W}_6$ at 1689°C result in a U-type reaction $L + \text{W} \leftrightarrow \text{CoAl} + \text{Co}_7\text{W}_6$ at 1490°C. From EPMA data it was found that the compound CoAl in that reaction contains 37.6 at.% Al, 56.8 at.% Co, 5.6 at.% W and the compound Co_7W_6 2.8 at.% Al, 48.2 at.% Co, 49 at.% W, whereas the W-base s.s. has the composition 1.8 at.% Al, 3.2 at.% Co, 95 at.% W. Compositions, which result in the primary formation of a Co-base s.s. are located in the region separated by the line e_1Ee_2 in the liquidus surface projection. The segment Ee_1 is the locus of ternary liquid composition in equilibrium with cobalt and CoAl in which the monovariant eutectic forms as seen in Fig. 2c, which shows fibrous shape CoAl and Co formed by eutectic solidification. The microstructure was obtained by deep-hole etching with a mixture of HF and HNO_3 . The segment Ee_2 is the locus of ternary liquid compositions in equilibrium with cobalt and Co_7W_6 . The microstructure shown in Fig. 2d may be rated as an argument for that eutectic formation.

Point E is the locus of a ternary eutectic at 1380°C. The composition of point E was shown to be 16.8 at.% Al, 68.4 at.% Co, 14.8 at.% W from the EPMA data. In the microstructure of the alloy shown in Fig. 2e there are a few primary grains of Co in the ternary eutectic (Co is etched).

The projection of the solidus surface of the Co–CoAl–W phase diagram is shown in Fig. 3. It involves four surfaces of solid phases: Co-base s.s. (γ), W-base s.s. (α), CoAl (β), Co_7W_6 (χ); two three-phase alloy fields ($\gamma + \beta + \chi$) and ($\beta + \chi + \alpha$), and five two-phase fields: ($\gamma + \beta$), ($\gamma + \chi$), ($\beta + \chi$), ($\chi + \alpha$), and ($\beta + \alpha$).

The boundary line of the Co-base s.s. solidus passes through a point of total aluminium and tungsten content 13.5 at.% Al, 10 at.% W at 1380°C. The

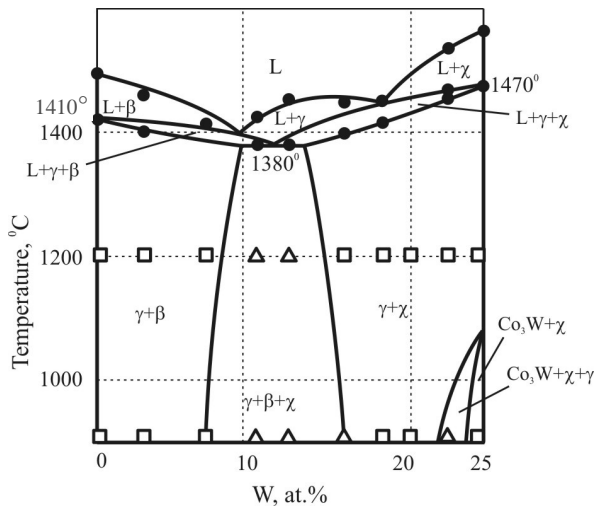


Fig. 4 Vertical section for the Co–CoAl–W system at 75 at.% Co. ● – single-phase alloys, □ – two-phase alloys, △ – three-phase alloys.

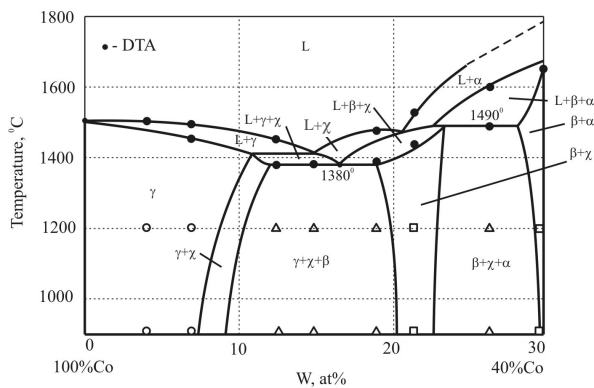


Fig. 5 Vertical section for the Co–CoAl–W system at equiatomic Al and W content. ● – single-phase alloys, □ – two-phase alloys, △ – three-phase alloys.

boundary line of the CoAl solidus reaches the point 30.4 at.% Al, 6.3 at.% W at this temperature, and from 37 at.% Al, 6 at.% W at 1490°C, when CoAl is in equilibrium with Co_7W_6 and W-base solid solution. The boundary line of the Co_7W_6 solidus passes through the point 3.4 at.% Al, 37 at.% W at 1380°C and from 2.8 at.% Al, 49 at.% W at 1490°C, according to the EPMA data.

The solidus temperature of the $(\text{CoAl}+\text{Co}_7\text{W}_6+\text{W})$ alloys was found to be 1490°C from DTA studies of annealed alloys and is the result of the invariant

reaction $\text{L}+\text{W}\leftrightarrow\text{CoAl}+\text{Co}_7\text{W}_6$. Fig. 2f shows the microstructure of an as-cast alloy. The composition of the W-base solid solution in this as-cast alloy was determined by EPMA as 1.8 at.% Al, 3.2 at.% Co, in equilibrium with CoAl containing 37.6 at.% Al, 5.6 at.% W, 56.8 at.% Co and Co_7W_6 containing 2.8 at.% Al, 49 at.% W, 48.2 at.% Co.

The two-phase solidus surfaces in the fusion diagram are connected to the boundary solidus lines of the primary solid solutions by tie-lines. Their solidus temperatures are slightly changed from 1410°C to 1380°C on the $(\text{Co}+\text{CoAl})$ solidus surface, from 1490°C to 1380°C on $(\text{CoAl}+\text{Co}_7\text{W}_6)$, from 1650°C to 1490°C on the $(\text{W}+\text{CoAl})$ solidus surface (in the investigated region), from 1470°C to 1380°C on $(\text{Co}+\text{Co}_7\text{W}_6)$ and from 1689°C to 1490°C on the $(\text{Co}_7\text{W}_6+\text{W})$ solidus surface.

Fig. 4 shows the vertical section for the Co–CoAl–W system at 75 at.% Co. It was constructed based on the constitution of the liquidus and solidus surfaces and the isothermal sections at 1200°C and 900°C. The solidus temperature for the invariant reaction $\text{L}\leftrightarrow\text{Co}+\text{CoAl}+\text{Co}_7\text{W}_6$ is close to the value for the binary eutectic reaction on the Co–Al side. The $(\text{Co}+\text{CoAl}+\text{Co}_7\text{W}_6)$ region expands with decreasing temperature and regions with Co_3W appear.

The vertical section with equal content of aluminum and tungsten is shown in Fig. 5.

References

- [1] E. Ganglberger, H. Novotny, F. Benesovsky, *Monatsh. Chem.* 96 (1965) 1658-1659.
- [2] G.P. Dmitrieva, T.S. Cherepova, A.K. Shurin, *Met. Sci. Treatm. Met.* 4 (2005) 3-6.
- [3] G.P. Dmitrieva, T.S. Cherepova, A.K. Shurin, *Met. Sci. Treatm. Met.* 2 (2006) 22-24.
- [4] L. Panteleymonov, E. Badtiev, L. Aleshina, *Vestn. Mosk. Univ. Ser. 2: Khim.* 15(1) (1974) 117-118.
- [5] Nagender Naidu, Sriramamurty, Rama Rao, *J. Alloy Phase Diagrams* 2 (1) (1986) 43-52.
- [6] T. Takemori, W.M. Yong, N. Taiji, *Trans. Jpn. Inst. Met.* 22 (5) (1981) 315-325.
- [7] A. Gabriel, H.L. Lukas, C.H. Allibert, I. Ansara, *Z. Metallkd.* 76(9) (1985) 589-595.
- [8] L. Kaufman, H. Neson, *Metall. Trans. A* 6(11) (1975) 2115-2122.